Title: The critical role of ASD-related gene *CNTNAP3* in regulating synaptic development and social behavior in mice

Authors: Da-li Tong[1, 3, #], Rui-guo Chen[2, 3, #], Yu-lan Lu[4], Wei-ke Li[1, 3], Yue-fang Zhang[1], Jun-kai Lin[1], Ling-jie He[1], Ting Dang[4], Shi-fang Shan[1], Xiao-Hong Xu[1], Yi Zhang[6], Chen Zhang[6], Ya-Song Du[5, *], Wen-Hao Zhou[4, *], Xiaoqun Wang[2, 3 *], Zilong Qiu[1, 3, *]

Affiliations:

[1] Institute of Neuroscience, State Key Laboratory of Neuroscience, CAS Center for Excellence in Brain Science and Intelligence Technology, Chinese Academy of Sciences, Shanghai, China, 200031

[2] Institute of Biophysics, State Key Laboratory of Brain and Cognitive Sciences, CAS Center for Excellence in Brain Science and Intelligence Technology; Chinese Academy of Sciences, Beijing 100101, China.

[3] The College of Life Science, University of Chinese Academy of Sciences, Beijing 100049, China.

[4] Department of Neonatology, Children's Hospital of Fudan University, Shanghai, China, 201102

[5] Shanghai Mental Health Center, Shanghai Jiao Tong University School of Medicine, Shanghai, China

[6] State Key Laboratory of Membrane Biology, PKU-IDG/McGovern Institute for Brain Research, School of Life Sciences; Peking University, Beijing, China

[#] These authors contribute equally to this work.

*Co-corresponding authors (zqiu@ion.ac.cn, xiaoqunwang@ibp.ac.cn, zwhchfu@126.com, yasongdu@163.com)

Abstract: Accumulated genetic evidences indicate that the contactin associated protein-like (CNTNAP) family is implicated in autism spectrum disorders (ASD). In this study, we identified transmitted genetic mutations in the *CNTNAP3* gene from Chinese Han ASD cohorts and Simons Simplex Collections. We found that CNTNAP3 interacted with synaptic adhesion proteins Neuroligin1 and Neuroligin2, as well as scaffolding proteins PSD95 and Gephyrin. Importantly, we found that CNTNAP3 plays an opposite role in controlling development of excitatory and inhibitory synapses *in vitro* and *in vivo*, in which ASD mutants exhibited *loss-of-function* effects. We showed that *Cntnap3*-null mice exhibited deficits in social interaction and spatial learning. These evidences elucidate the pivotal role of CNTNAP3 in synapse development and social behavior, providing the mechanistic insights for ASD.

One Sentence Summary: *CNTNAP3* is a candidate gene for ASD.

Main Text:

Autism spectrum disorder (ASD) is a prevalent neurodevelopmental disorder with early onset during childhood, characterized by deficits in social interaction and stereotypic behaviors. Numerous genes were discovered to be involved in ASD by human genetic studies (*1-3*). Particularly, mutations in genes encoding synaptic adhesion and cytoskeleton molecules, including Neuroligin (NLGN), Neurexin (NRXN) and SHANK family members, are often found in ASD patients, suggesting that the synaptic dysfunction significantly contribute to ASD (*4-7*).

The contactin associated protein-like (CNTNAP) family (also known as the CASPR protein family), containing 5 members from CNTNAP1 to CNTNAP5, is structurally close to the Neurexin

(NRXN) family, featured by multiple repeats of epidermal growth factor (EGF) domains and laminin G (LamG) domains in the extracellular domains, as well as the intracellular PDZ-binding domain (*8-11*). CNTNAP1 and CNTNAP2 are involved in the formation of myelin and trafficking potassium channels to the cell membrane (*12-14*). Genetic evidences indicated strong connections between the *CNTNAP2* gene with ASD (*15-17*). The CNTNAP2 protein plays a critical role in neural development and synaptic transmission, and *Cntnap2* null mice displayed various autistic-like behaviors (*18*, *19*). CNTNAP4 is critical for the formation of axo-axonic synapse by interacting with Contactin5 in the peripheral nervous system (*20*). Whereas in the central nervous system, CNTNAP4 plays a specific role in regulating synaptic transmission of GABAergic neurons. Moreover, the *Cntnap4* knockout mice also showed heavily stereotypic behaviors such as self-grooming (*21*).

Identification of *CNTNAP3* mutations in ASD patients

In a whole-exome sequencing study for 120 ASD patients collected in Shanghai Mental Health Hospital (*22*), we found that there are two probands (ASD22, ASD652) carrying the same inherited mutation (causing amino acid alternation P614A) in the *CNTNAP3* gene, validated by Sanger sequencing (Fig. 1A, Fig. S1A, B). We identified another proband featured "Human phenotype ontology (HPO): autism" in the database for brain disorders patients in Fudan Children's Hospital of Shanghai, in whom one inherited mutation (R786C) transmitted from father in the *CNTNAP3* gene were found, suggesting the connection between *CNTNAP3* and ASD (Fig. 1B, Fig. S1C).

To determine whether there may be *CNTNAP3* mutations in ASD populations from different geographic regions, we next searched the Simons simplex collections (SSC) and found 2 ASD

probands carrying R786H mutation in the *CNTNAP3* gene, among 2600 ASD trios, both of which are inherited from unaffected mothers (Fig. 1C). We further examined the mutation rates of *CNTNAP3* mutations (P614A, R786C and R786H) in the gnomAD database (http://gnomad.broadinstitute.org). P614A and R786C exhibited extremely low occurrence (less than 0.01%) in total 245686 populations of the gnomAD database, indicating that they are rare variants. The R786H mutation occurs 0.012% in gnomAD database, which is still much lower than it in SSC (2/2600, 0.077%), suggesting the possible enrichment of R786H mutation in ASD cohorts. The R786 localize in the LamG domains, and P614 is within fibrinogen-related domain (FRed) domain (Fig. 1D, E).

CNTNAP3 interacts with NLGNs and NRXNs

To investigate the role of CNTNAP3 in brain development, we first examined the expression profile of CNTNAP3 in developmental stages and various regions in mouse brain via quantitative PCR (Fig. 1F, G), due to lack of suitable antibody against the mouse CNTNAP protein. We found that CNTNAP3 was highly expressed in cortex and hippocampus of the mouse postnatal brain (Fig. 1F; Fig. S1D, E) and had relative low expression levels in cerebellum and spinal cord (Fig. 1G). We further performed *in situ* hybridization using probes again the mouse CNTNAP3 together with immunostaining using various cell markers in cortex and hippocampus to determine the expression pattern of CNTNAP3 in different neuronal cell types (Fig. 1H, Fig. S2A; sense probe controls of *in situ* hybridization shown in Fig. S2B). Interestingly, we found that majority (~70%) of CNTNAP3-expressing neurons are co-localized with vesicular glutamate transporter 1 (vGlut1) protein in cerebral cortex, whereas around 10% CNTNAP3-expressing neurons are parvalbumin-

positive, indicating that CNTNAP3 is mainly expressed in glutamatergic neurons in cortex (Fig. 1I).

Structurally similar with NRXN superfamily proteins, CNTNAP3 has repeated LamG domains and EGF domains, as well as an intracellular PDZ-binding domain (Fig. 1D), thus we would like to determine whether CNTNAP3 may interact with synaptic adhesion molecules, such as Neuroligin1 (NLGN1) and Neuroligin 2 (NLGN2), as well as synaptic scaffolding proteins. We constructed a plasmid expressing hemagglutinin (HA)-tagged full-length human CNTNAP3. To address which domain would be responsible for interaction, besides full-length CNTNAP3, we also made the plasmid expressing only one extracellular LamG domain and the intracellular PDZ-binding domain of CNTNAP3 protein (C3-LamG) (Fig. 1E).

By the co-immunoprecipitation experiment, we found the CNTNAP3 interacted with both NLGN1 and NLGN2 (Fig. 1J, K). Deletion of extracellular LamG domains (C3-LamG) significantly weaken, but not diminish the interaction, suggesting that only one LamG domain is sufficient for interaction between CNTNAP3 with NLGN1 or NLGN2 (Fig. 1J, K). Furthermore, we found that CNTNAP3 also interacted with synaptic scaffolding proteins, including PSD-95 and Gephyrin but not SHANK3 (Fig. 1L; Fig. S3A). As NLGN1 and PSD-95 primarily located in the post-synaptic compartment of excitatory synapse, whereas NLGN2 and Gephyrin localized in the inhibitory synapses, these evidences suggest that CNTNAP3 may exist in both excitatory and inhibitory synapses.

CNTNAP3 regulates excitatory and inhibitory synapse development differentially

To assess the function of CNTNAP3 in synaptic development, we constructed the short hairpin RNA (shRNA) against the mouse *Cntnap3* gene and confirmed the efficiency of down-regulating the endogenous expression level of *Cntnap3* (Fig. S3B). We next investigate whether knockdown of *Cntnap3* may affect neuronal morphology and synaptic development in cultured mouse primary neurons. We transfected GFP expressing plasmids, together with control vector, *Cntnap3* shRNA, human WT *CNTNAP3* cDNA as well as human *CNTNAP3* cDNA carrying ASD-related mutations, respectively. Since mouse *Cntnap3* shRNA does not target human *CNTNAP3*, human WT *CNTNAP3* cDNA could serve as a rescue construct for shRNA knockdown. We found that knockdown of CNTNAP3 expression led to significantly decrease of axonal and dendritic length, as well as dendritic branch number (Fig. 2A, B, C, D, E). Importantly, although human WT *CNTNAP3* cDNA was able to fully restore axonal and dendritic length to normal level after shRNA knockdown, two ASD-related mutations (P614A, R786C) were not able to rescue defects caused by *Cntnap3* shRNA, exhibiting *loss-of-function* effects (Fig. 2B, D, E).

Next, we would like to investigate whether CNTNAP3 contributes to synaptic development. After transfections of GFP expressing plasmids, along with vector control, or *Cntnap3* shRNA, as well as *Cntnap3* shRNA with human WT *CNTNAP3* or ASD-related mutations, respectively in mouse primary cortical neurons *in vitro* for 14 days, we then measured amounts of excitatory synapses by anti-vesicular glutamate transporter 1 (vGlut1) immunostaining and numbers of inhibitory synapses by anti-vesicular GABA transporter (vGat) immunostaining onto the GFP-expressing neurons transfected with either control vectors or various manipulations (Fig. 2F). We found that knockdown of *Cntnap3* led to decrease of excitatory synapse formation which were fully rescued by WT CNTNAP3, but not the P614A and R786C mutants (Fig. 2F, G). Interestingly,

inhibitory synapse numbers measured by anti-vGat staining, were increased after knockdown of CNTNAP3, which could be fully rescued to normal level by WT and R786C, but not P614A mutant, suggesting that CNTNAP3 may play a negative role in repressing formation of inhibitory synapse and P614A may exhibit *loss-of-function* effects in this regard. Furthermore, numbers of spine were also markedly decreased in the CNTNAP3 knockdown group, which were restored to the normal level when co-expressed with WT CNTNAP3, but not P614A and R786C mutants (Fig. 2I). These evidences indicate that CNTNAP3 may promote excitatory glutamatergic synapse formation, whereas inhibit GABAergic synapse formation. Moreover, ASD-related mutations may exhibit *loss-of-function* effects regarding to excitatory and inhibitory synapses formation specifically.

CNTNAP3 regulates development of excitatory synapse and PV-positive inhibitory neurons *in vivo*

To address the role of CNTNAP3 *in vivo*, we constructed *Cntnap3*$^{-/-}$ mouse by CRISPR/Cas9 technology and conditional knockout of *Cntnap3* mouse by flanking exon 3 with LoxP cassettes with homology recombination strategy (Fig. S3C, D). We first examined whether development of excitatory synapses may be altered in *Cntnap3*$^{-/-}$ mice, by measuring the morphology of dendritic spine of pyramidal neurons in hippocampal CA1 region using Golgi staining. We found that spine density of hippocampal CA1 neurons significantly decreased in *Cntnap3*$^{-/-}$ mice in comparison with WT mice, suggesting that CNTNAP3 plays a critical role for excitatory synapse development *in vivo* (Fig. 3A, B). Next, we crossed *Nex-Cre* mice with *Cntnap3* $^{flox/flox}$ mice to specifically delete *Cntnap3* in excitatory neurons (*23*). In *Nex-Cre: Cntnap3* $^{flox/flox}$ mice, spine density also dramatically decreased in hippocampal CA1 neurons comparing to WT mice, indicating that

CNTNAP3 likely regulates development of excitatory synapse through cell-autonomous manner (Fig. 3C, D).

Strikingly, we found that parvalbumin (PV)-positive GABAergic neurons markedly increased in cortical regions and hippocampus of *Cntnap3*$^{-/-}$ mice in comparison with WT mice (Fig. 3E, F, G). But somatostatin (SST)-positive GABAergic neurons remained unaffected in *Cntnap3*$^{-/-}$ mice (Fig. S4A, B, C). These data suggest that CNTNAP3 may hamper development of PV-positive subtype of GABAergic neurons.

CNTNAP3 regulates excitatory and inhibitory synaptic transmission *in vivo*

To determine the role of CNTNAP3 in synaptic transmission *in vivo*, the whole-cell patch clamp recording was performed on the hippocampal CA1 neurons and layer 5 neurons of neocortex in acute slice preparations of *Cntnap3*$^{-/-}$ mice and WT mice as control (Fig. 4A). We firstly measured passive electrical properties of these cells, including resting membrane potential (RMP), input resistance (R_{in}) and membrane capacity (Cm) (Fig. 4B, C, D). Our results showed that intrinsic properties of neurons in layer 5 of *Cntnap3*$^{-/-}$ mice were equivalent to their counterparts in control mice (The upper panel of Fig. 4B, C, D). However, hippocampal CA1 pyramidal neurons of *Cntnap3*$^{-/-}$ mice appeared more depolarized compared to the cells in WT mice (The lower panel of Fig. 4B). Moreover, the R_{in} was elevated and the Cm decreased in *Cntnap3*$^{-/-}$ mice comparing to WT mice (The lower panel of Fig. 4C, D). These results suggest that membrane properties and ion channel distributions may be altered in hippocampal CA1 neurons in *Cntnap3*$^{-/-}$, due to lack of *Cntnap3*.

These developmental changes may further shape properties of action potentials and membrane activities. We thus investigated the inward and outward current during the excitation of neurons evoked by a series of voltage pulses in cortical layer 5 and hippocampal CA1 neurons of *Cntnap3*$^{-/-}$ and WT mice (Fig. 4E). We found that amplitude of inward currents of both layer 5 and CA1 neurons significantly decreased in *Cntnap3*$^{-/-}$ mice compared to those in WT mice (Fig. 4F). The outward currents displayed the same tendency (Fig. 4G). These results suggested that knockout of *Cntnap3* altered excitability of cortical and hippocampal neurons. However, when we measured firing rate and amplitude of action potentials of cortical layer 5 and hippocampal CA1 neurons, we found that these properties were not influenced by knockout of *Cntnap3* (Fig. S5A-F). We reasoned that the altered excitability did not lead to change of fire rate may be due to the input of these neurons were also changed in the absence of *Cntnap3*.

Therefore, to elucidate the role of CNTNAP3 in synapse development, we further examine excitatory and inhibitory synaptic transmission in the hippocampal CA1 region of *Cntnap3*$^{-/-}$ mice. We measured miniature excitatory postsynaptic currents (mEPSC) and miniature inhibitory postsynaptic current (mIPSC) in the presence of tetrodotoxin (TTX) in acute hippocampal slices of *Cntnap3*$^{-/-}$ and WT mice (Fig. S5G, Fig. 4H, K). We found that the frequency, but not amplitude, of mEPSC significantly decreased in adult *Cntnap3*$^{-/-}$ mice, in consistent with the observation of decreased excitatory synapse development *in vitro* and reduced spine density *in vivo* (Fig. 4I, J). Interestingly, both amplitude and frequency of mIPSC significantly increased in the hippocampal CA1 region of adult *Cntnap3*$^{-/-}$ mice, suggesting that numbers and strength of inhibitory synapses are both increased in *Cntnap3*$^{-/-}$ mice (Fig. 4L, M). We also measured mEPSC and mIPSC in adolescent mice from postnatal day 14 (P14) to 28 (P28) (Fig. S5H, I). The frequency of mEPSC

in *Cntnap3*$^{-/-}$ adolescent mice was significantly decreased (Fig. S5J, K), whereas the frequency of mIPSC was markedly increased (Fig. S5L, M). These results suggest that CNTNAP3 also play a pivotal role in regulating excitatory and inhibitory synaptic transmission *in vivo*. Taken together, these evidences indicate that CNTNAP3 regulates intrinsic neuronal excitability, as well as playing an opposite role in controlling development of excitatory and inhibitory synapses *in vivo*.

Defects in social interaction and cognition in *Cntnap3*$^{-/-}$ mice

Finally, we would like to determine whether deletion of *Cntnap3* may lead to autistic-like behavioral abnormalities in mouse, although previous studies showed that *Cntnap3*$^{-/-}$ mice exhibited the normal motor function and anxiety level (*24*). We performed a battery of behavioral tasks on *Cntnap3*$^{-/-}$, excitatory (*Nex-Cre: Cntnap3*$^{flox/flox}$) and inhibitory (*Vgat-ires-Cre: Cntnap3*$^{flox/flox}$*)* specific knockout mice. Remarkably, in the three-chamber test, *Cntnap3*$^{-/-}$ mice appeared no preference in staying with mouse over an empty cage, while still exhibited increased interaction time with novel mice over familiar mice, suggesting that *Cntnap3*$^{-/-}$ showed defects in social interactions (Fig. 5A, B, Fig. S6A). Interestingly, we found that *Nex-Cre: Cntnap3*$^{flox/flox}$ mice, specific deletion of *Cntnap3* in excitatory neurons, showed no defects in recognizing either mice over cage, or novel over familiar mice (Fig. 5C, D, Fig. S7A). However, inhibitory neuron specific knockout mice, *Vgat-ires-Cre: Cntnap3*$^{flox/flox}$, exhibited defects in distinguishing novel mice with familiar mice, suggesting that *Cntnap3* in inhibitory neurons may contribute to social memory (Fig. 5E, F, Fig. S9A).

Next, we used the Barnes Maze test to examine whether *Cntnap3*$^{-/-}$ mice may have defects in learning and memory tasks. First, we found that *Cntnap3*$^{-/-}$ mice spent significantly longer time

and more error holes to find the correct hole during the training session, suggesting that the learning ability in *Cntnap3*$^{-/-}$ mice was compromised (Fig. 5G, H). We then performed the short-term and long-term memory tasks at day 5 and day 12 after training, respectively. We found that *Cntnap3*$^{-/-}$ mice spent markedly increased error holes and latency time in both memory tests, indicating the both short- and long-term memory capacity of *Cntnap3*$^{-/-}$ mice are severely affected (Fig. 5I-L, Fig. S6B, C). We found no defects of *Cntnap3*$^{-/-}$ mice in consequent series of tests, including elevated platform maze (Fig. S6D, E), light/dark shuttling (Fig. S6F), open field test (Fig. S6G, H), novel object recognition (Fig. S6I), as well as context and cue-dependent fear conditioning (Fig. S6J, K, L). These data suggest that *Cntnap3*$^{-/-}$ mice have specific defects related to social behaviors, as well as learning and memory, but appeared normal levels of anxiety and fear conditioning responses.

In the excitatory neuron specific knockout mice (*Nex-Cre: Cntnap3*$^{flox/flox}$) and inhibitory neuron specific knockout mice (*Vgat-ires-Cre: Cntnap3*$^{flox/flox}$), we found similar defects in learning curve of the Barnes Maze test (Fig. S7B, C, Fig. S9B, C), suggesting that proper functions of CNTNAP3 in both excitatory and inhibitory neurons are required for acquiring a certain type of spatial memory. Interestingly, deletion of CNTNAP3 in excitatory neurons exhibited more severe defects in long-term and short-term memory tasks, comparing to inhibitory neurons specific deletion (Fig. S7D-I, Fig. S9D-I), suggesting that CNTNAP3 may play a more important role in glutamatergic neurons in regulating long-term memory maintenance. Similarly, we did not find any defects in the elevated platform maze and open field test in either excitatory neuron knockout (Fig. S8 A-D), or inhibitory neurons knockout mice (Fig. S10A-D), suggesting that CNTNAP3 has no effects in regulating anxiety levels.

Discussion

Taken together, we characterized critical functions of a synaptic adhesion molecule CNTNAP3 in synaptic development and transmission, as well as social behaviors and cognitive tasks. The genetic connections between CNTNAPs family with ASD is very intriguing over the years, as other synaptic adhesion molecules are implicated in ASD. In this study, we identified two transmitted mutations (P614A, R786C) in *CNTNAP3* gene through whole-exome sequencing. Although none of mutations are *de novo* mutations, we further address the functions of each mutations in regarding to synapse development and showed that they are indeed *loss-of-function* variants. These data suggest that transmitted variants in ASD patients could also significantly contribute to pathophysiology of ASD.

Although *CNTNAP2* and *CNTNAP4* are ASD candidate genes from previous genetic and functional studies, the detail function of CNTNAPs in synapse development is yet to be determined. The finding that CNTNAP3 interacted with NLGN1/2 family members strongly suggest that CNTNAP3 is an important synaptic adhesion molecules that plays critical roles in regulating synapse development, as showed in this study (*25*, *26*). Our data suggest that CNTNAP3 is an essential component of excitatory synapse and inhibitory synapse. Further work is needed to determine the molecular mechanisms underlying the differentially regulatory function of CNTNAP3 for both excitatory and inhibitory synapses. The finding that CNTNAP3 regulates synapses development differentially provides novel insights for further understanding the synapse basis for ASD.

Comparing with behavioral defects identified in *Cntnap2*$^{-/-}$ and *Cntnap4*$^{-/-}$ mice, we found rather specific defects in social behaviors and cognitive tasks in *Cntnap3*$^{-/-}$ mice, suggesting that CNTNAP3 may play a more specific role in regulating social interaction, as well as learning and memory in mice. Further work of determining specific neural circuits responsible for defects in social behaviors and learning memory would be crucial to provide insights into neural circuits regulating different cognitive behaviors specifically. Combined with the genetic mutations we discovered in Chinese Han ASD and Simons simplex collections, as well as functional evidences in genetic engineered mice, we suggest that *CNTNAP3* is a ASD candidate gene and the imbalance of excitatory and inhibitory synapse development caused by mutations of *CNTNAP3* contribute to the abnormal social behaviors and cognitive functions.

References and notes

1. G. Huguet, E. Ey, T. Bourgeron, *Annu Rev Genomics Hum Genet* **14**, 191 (2013-01-20, 2013).
2. A. J. Willsey, M. W. State, *CURR OPIN NEUROBIOL* **30**, 92 (2015-02-01, 2015).
3. L. de la Torre-Ubieta, H. Won, J. L. Stein, D. H. Geschwind, *NAT MED* **22**, 345 (2016-04-01, 2016).
4. P. Szatmari *et al.*, *NAT GENET* **39**, 319 (2007-03-01, 2007).
5. J. Feng *et al.*, *NEUROSCI LETT* **409**, 10 (2006-11-27, 2006).
6. S. Jamain *et al.*, *NAT GENET* **34**, 27 (2003-05-01, 2003).
7. H. G. Kim *et al.*, *AM J HUM GENET* **82**, 199 (2008-01-01, 2008).
8. I. Spiegel, D. Salomon, B. Erne, N. Schaeren-Wiemers, E. Peles, *MOL CELL NEUROSCI* **20**, 283 (2002-06-01, 2002).
9. H. J. Bellen, Y. Lu, R. Beckstead, M. A. Bhat, *TRENDS NEUROSCI* **21**, 444 (1998-10-01, 1998).
10. E. Peles *et al.*, *EMBO J* **16**, 978 (1997-03-03, 1997).
11. W. Traut, D. Weichenhan, H. Himmelbauer, H. Winking, *MAMM GENOME* **17**, 723 (2006-07-01, 2006).
12. J. C. Rios *et al.*, *J NEUROSCI* **20**, 8354 (2000-11-15, 2000).
13. M. Traka *et al.*, *J CELL BIOL* **162**, 1161 (2003-09-15, 2003).

14. S. Poliak *et al.*, *J CELL BIOL* **162**, 1149 (2003-09-15, 2003).

15. M. Alarcon *et al.*, *AM J HUM GENET* **82**, 150 (2008-01-01, 2008).

16. D. E. Arking *et al.*, *AM J HUM GENET* **82**, 160 (2008-01-01, 2008).

17. B. Bakkaloglu *et al.*, *AM J HUM GENET* **82**, 165 (2008-01-01, 2008).

18. O. Penagarikano *et al.*, *CELL* **147**, 235 (2011-09-30, 2011).

19. G. R. Anderson *et al.*, *Proc Natl Acad Sci U S A* **109**, 18120 (2012-10-30, 2012).

20. S. Ashrafi *et al.*, *NEURON* **81**, 120 (2014-01-08, 2014).

21. T. Karayannis *et al.*, *NATURE* **511**, 236 (2014-07-10, 2014).

22. Z. Wen *et al.*, *MOL AUTISM* **8**, 43 (2017-01-20, 2017).

23. A. H. Kashani *et al.*, *J NEUROSCI* **26**, 8398 (2006-08-09, 2006).

24. H. Hirata, A. Takahashi, Y. Shimoda, T. Koide, *PLOS ONE* **11**, e147887 (2016-01-20, 2016).

25. B. Chih, H. Engelman, P. Scheiffele, *SCIENCE* **307**, 1324 (2005-02-25, 2005).

26. F. Varoqueaux *et al.*, *NEURON* **51**, 741 (2006-09-21, 2006).

27. K. Tabuchi *et al.*, *SCIENCE* **318**, 71 (2007-10-05, 2007).

28. S. Jamain *et al.*, *Proc Natl Acad Sci U S A* **105**, 1710 (2008-02-05, 2008).

Acknowledgments

We thank the team of WuXi NextCODE for technical assistance in SSC data analysis. This work was supported by the National Basic Research Program of China (2014CB964600, 2017YFA0105201, 2017YFA0103303, 2017YFA0102601), NSFC Grants (#31625013, #91732302, #81527901, #81471484, #31670842). the Strategic Priority Research Program of the Chinese Academy of Sciences (XDA01020309), and Shanghai Brain-Intelligence Project from STCSM (16JC1420500). The research is supported by the Open Large Infrastructure Research of Chinese Academy of Sciences. We appreciate obtaining access to genotype, phenotype and

pedigree data on SFARI Base. The authors declare that they do not have any conflicts of interest for this work.

Figure 1 Tong et al.

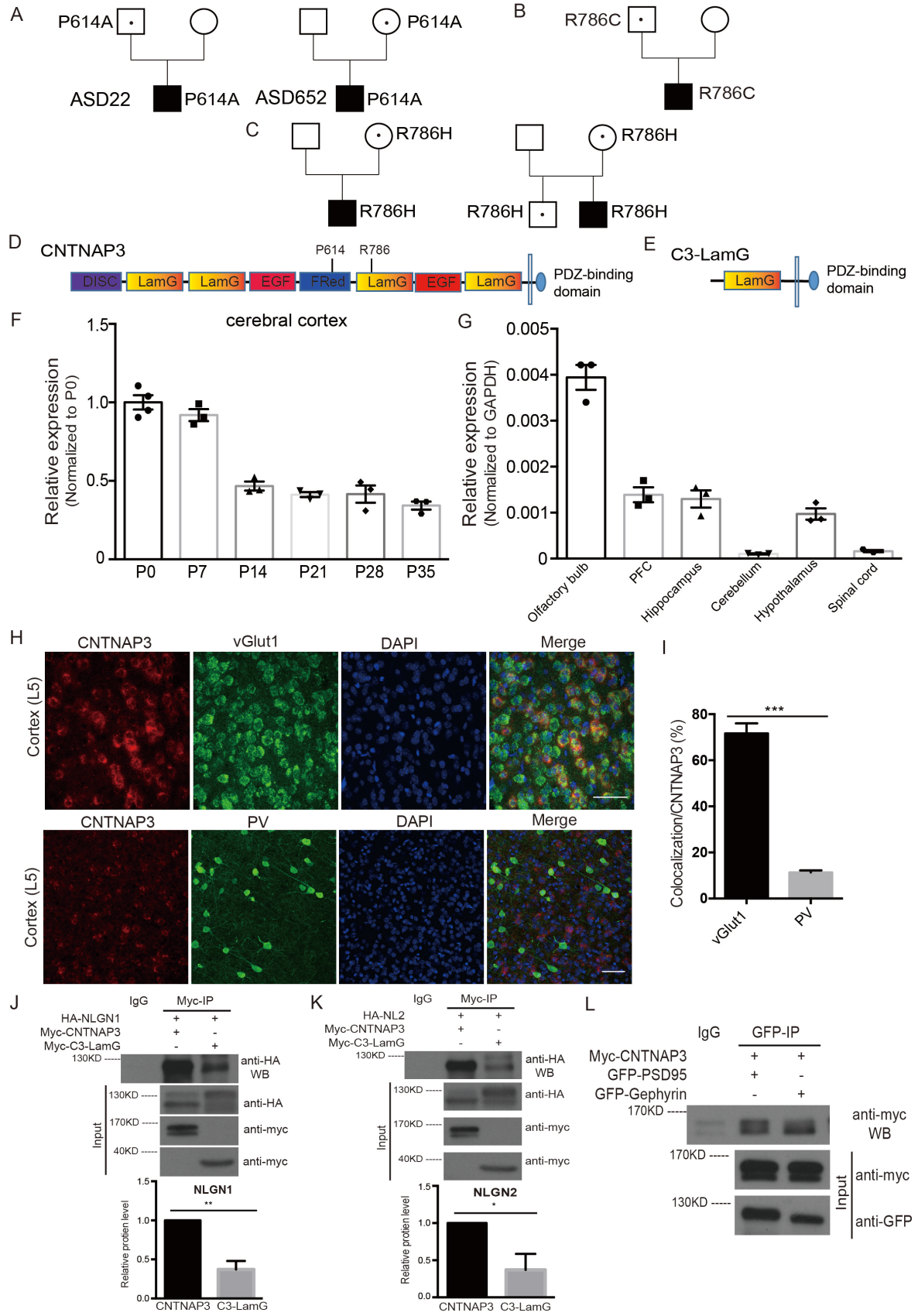

Figure 1. ASD-related *CNTNAP3* mutations and the expression pattern of *Cntnap3* in mouse brain.

(A) *CNTNAP3* mutations found in the ASD patients. Inherited mutations of P614A was found in ASD22 and ASD652 trios. (B) Transmitted mutations of R786C was found in father and the proband. (C) Inherited mutations of R786H were found in SSC cases. (D) The schematic structure and locations of P614 and R786 in the CNTNAP3 protein. (E) The schematic structure of CNTNAP3-LamG (C3-LamG for short). (F) Expression levels of *Cntnap3* in cerebral cortex of mouse in different ages (C57BL/6). (G) Expression levels of *Cntnap3* in different regions of the CNS of mouse (C57BL/6, Postnatal 28 days: P28). (H) Double labeling with immunostaining and *in situ* hybridization on P14 wild-type cortex with co-localization of CNTNAP3 (*in situ*, red) and vGlut1 (*in situ*, green) or PV (immunostaining, green). (I) Mean percentage of co-localization of CNTNAP3 and vGlut1 or PV (co-localization / CNTNAP3 positive). (J) Co-immunoprecipitation of myc-CNTNAP3, myc-C3-LamG and HA-NLGN1 in 293T cells. Immunoprecipitated (IP) with anti-myc antibody, immunoblotted (IB) with anti-myc and anti-HA antibodies. (K) Co-immunoprecipitation of myc-CNTNAP3, myc-C3-LamG and HA-NLGN2 in 293T cells. IP with anti-myc antibody, IB with anti-myc and anti-HA antibodies. (L) Co-immunoprecipitation of GFP-PSD95, GFP-Gephyrin, and myc-CNTNAP3 in 293T cells. IP with anti-GFP antibody, IB with anti-myc and anti-GFP antibodies. (H, I, mouse number n = 3, Scale bar: 50μm.) Statistical significance was evaluated by Student's *t* test: * $p < 0.05$, ** $p < 0.01$; error bars, ± SEM.

Figure 2 Tong et al.

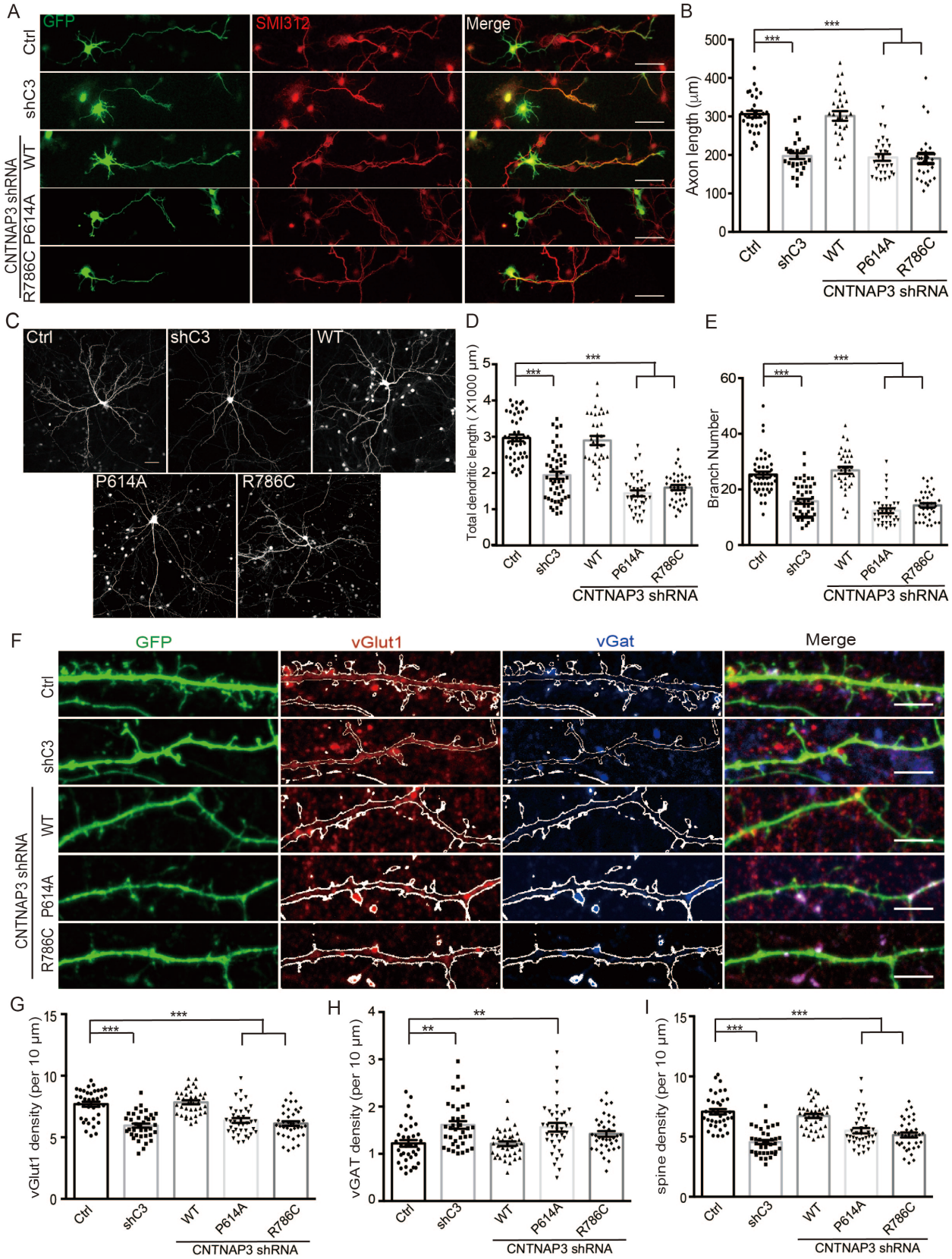

Figure 2. CNTNAP3 regulated neurite and synapse development.

(A) Immunostaining of GFP (green) and SMI-312 (red) in cultured mouse embryonic 14.5 cortex neurons. The neurons were transfected with *Cntnap3* shRNA (shC3) or DsRed shRNA (Ctrl) and were rescued by human WT CNTNAP3, P614A or R786C mutant. (E14.5+DIV 3, Scale bar: 50μm) (B) Quantitative analysis of axon length in (A) (counted cell numbers Ctrl: n=31, shC3: n=29, WT: n=30, P614A: n=29, R786C: n=26.). (C) Immunostaining of GFP (green) in cultured E14.5 cortex neurons. (E14.5+DIV 14, Scale bar: 50μm) (D) Dendritic length analysis of (C). (counted neuron numbers Ctrl: n=46, shC3: n=50, WT: n=35, P614A: n=36, R786C: n=36.) (E) Branch numbers analysis in (C). (F) Immunostaining of GFP (green), vGlut1 (red) and vGat (blue) in cultured E14.5 cortex neurons. (E14.5+DIV 14, counted cell numbers n=37 for each group. Scale bar: 5μm) (G) Quantitative analysis of vGlut density in (F). (H) Quantitative analysis of vGat density in (F). (I) Quantitative analysis of spine density in (F). Statistical significance was evaluated by one-way ANOVA: *$p < 0.05$, ** $p < 0.01$, *** $p < 0.001$. Error bars, ±SEM.

Figure 3 Tong et al.

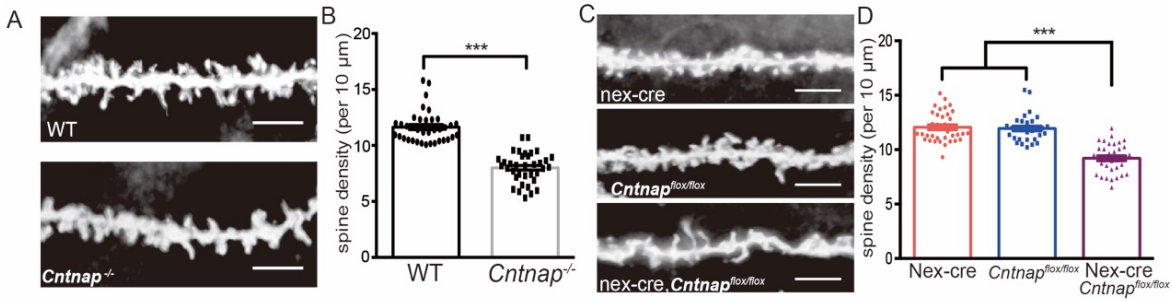

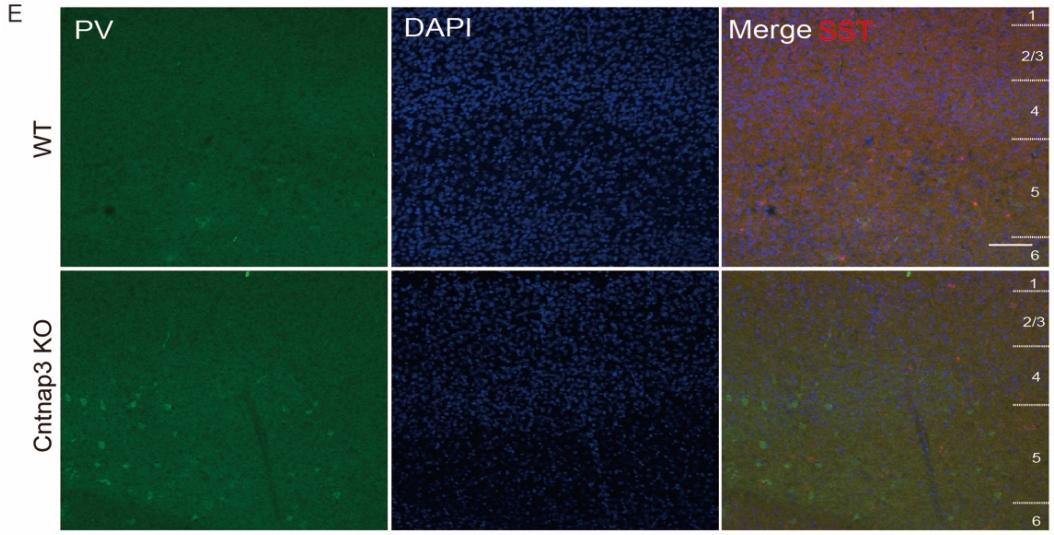

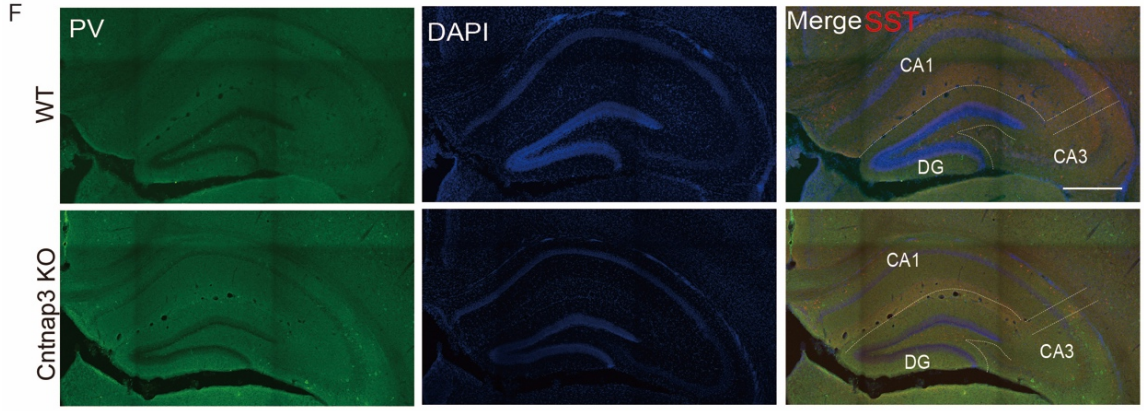

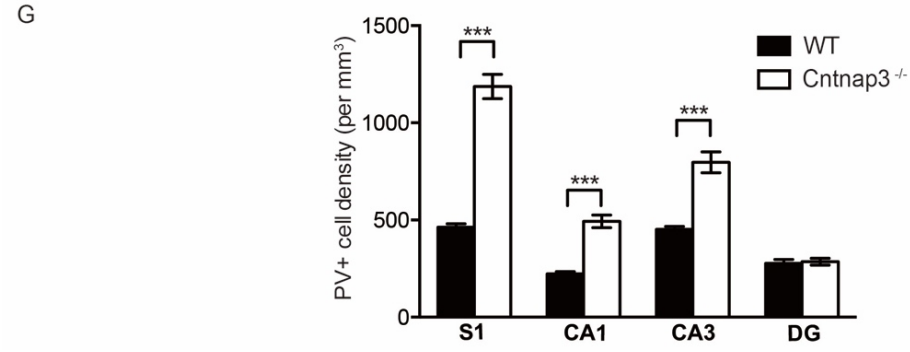

Figure 3. *Cntnap3*$^{-/-}$ mice showed decreased spine density and increased PV-positive neurons in cortex and hippocampus.

(A) Golgi staining in adult *Cntnap3*$^{-/-}$ mice in CA1 region. (apical dendrite, 2-4 months of age, mice number n=3 for either WT or KO, scale bar: 5μm) (B) Quantitative analysis of spine density in *Cntnap3*$^{-/-}$ mice. (neuron numbers, WT: n=37, *Cntnap3*$^{-/-}$: n=36) (C) Golgi staining in adult *Nex-Cre:Cntnap3*$^{flox/flox}$ mice in CA1 region. (apical dendrite, from 2-4 months of age, mice number n=3 for each genotype, scale bar: 5μm) (D) Quantitative analysis of spine density in *Nex-Cre:Cntnap3*$^{flox/flox}$ mice. (neuron numbers *Nex-Cre*: n=36, *Cntnap3*$^{flox/flox}$: n=30, *Nex-Cre:Cntnap3*$^{flox/flox}$: n=34, mice number n=3 for each genotype) (E) Immunochemistry of PV (green) and SST (red) in S1 (primary somatosensory cortex) region of *Cntnap3* KO mice at postnatal 14 days of age (P14). (Scale bar: 250μm) (F) Immunochemistry of PV (green) and SST (red) in hippocampus region of P14 *Cntnap3*$^{-/-}$ mice. (Scale bar: 250μm) (G) Quantitative analysis of density of PV positive neurons in *Cntnap3*$^{-/-}$ mice. (mice number, n=3 for WT and KO) Statistical significance was evaluated by Student's *t* test (*Cntnap3*$^{-/-}$ vs. WT) or one-way ANOVA (*Nex-Cre:Cntnap3*$^{flox/flox}$ vs. other groups): ***$p < 0.001$. Error bars, ± SEM.

Figure 4 Tong et al.

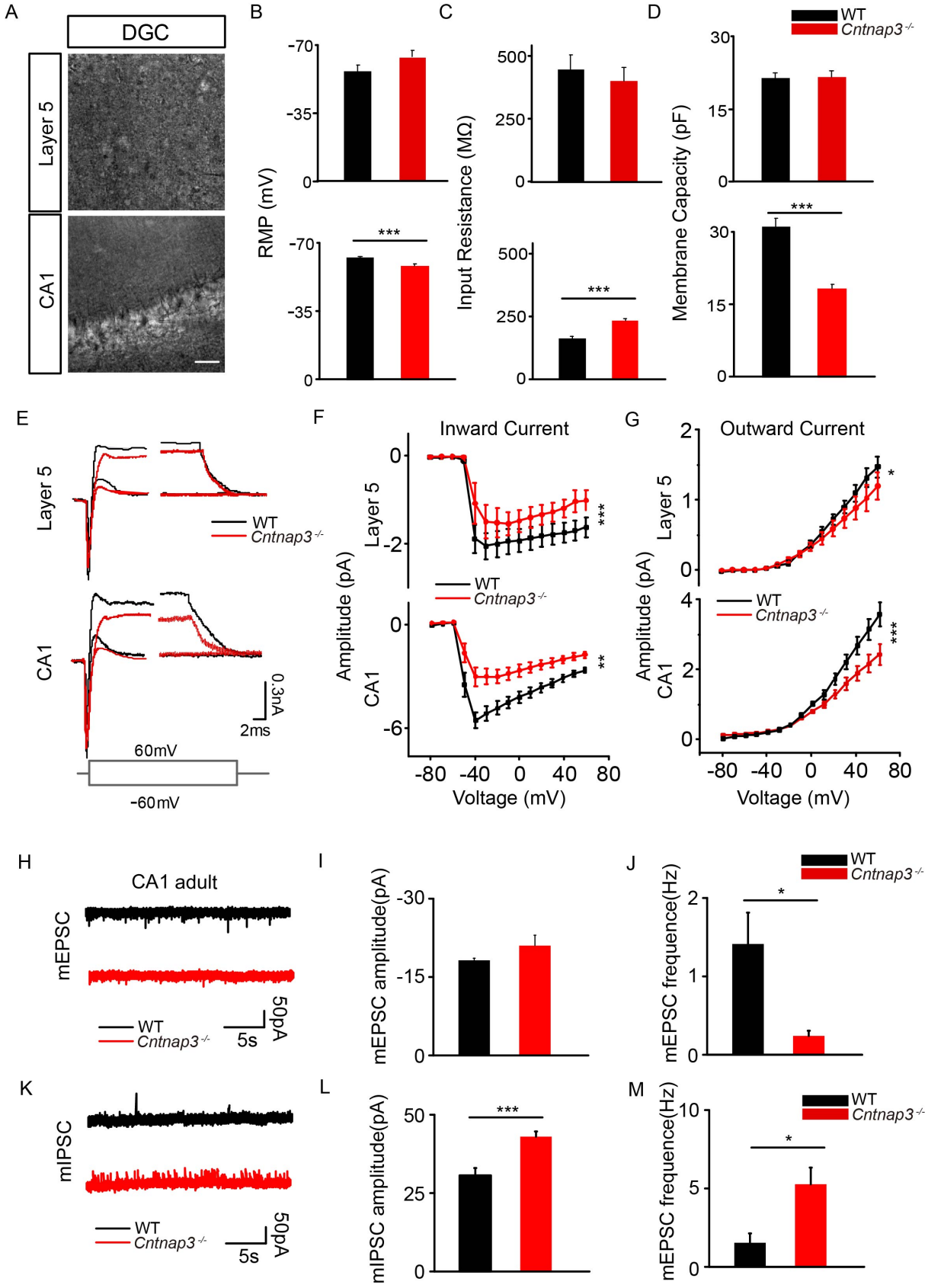

Figure 4. *Cntnap3*$^{-/-}$ mice exhibited decreased mEPSC and increased mIPSC frequency in hippocampal CA1 neurons.

(A) Images of whole-cell recording of cortical layer 5 and hippocampal CA1 neurons in bright field, scale bars: 50 μm. Resting membrane potential (B), input resistance (C) and membrane capacity (D) of neurons in cortical layer 5 (upper panel, 29 cells from 3 WT mice, 26 cells from 3 KO mice) and hippocampal CA1 (lower panel, 38 cells from 4 WT mice, 39 cells from 4 WT mice). (E) Representative current responses of neurons in cortical layer 5 and hippocampal CA1 at -60mV and 60 mV. Amplitude of inward current (F) and outward current (G) responses of neurons in cortical layer 5 (upper panel, inward current: 26 traces from 3 WT mice, 21 traces from 3 KO mice, outward current: 29 traces from 3 WT mice, 26 traces from 3 KO mice) and hippocampal CA1 (lower panel, inward current: 32 traces from 4 WT mice, 33 traces from 4 KO mice, outward current: 38 traces from 4 mice, 33 traces from 4 KO mice) evoked by a series of voltage steps. (H) Representative mEPSC traces of neurons of hippocampal CA1 in *Cntnap3*$^{-/-}$ and WT adult mice. Amplitude (I) and frequency (J) of mEPSC of hippocampal CA1 in KO and WT adult mice (16 traces from 4 WT mice, 18 traces from 4 KO mice). (K) Representative mIPSC traces of neurons of hippocampal CA1 in KO and WT adult mice. Amplitude (L) and frequency (M) of mIPSC of hippocampal CA1 in KO and WT adult mice (20 traces from 4 WT mice, 20 traces from 4 KO mice). Statistical significance was evaluated by Student's t test or two-way ANOVA (curve): * $p < 0.05$; ** $p < 0.01$; *** $p < 0.001$. Error bars, ± SEM.

Figure 5 Tong et al.

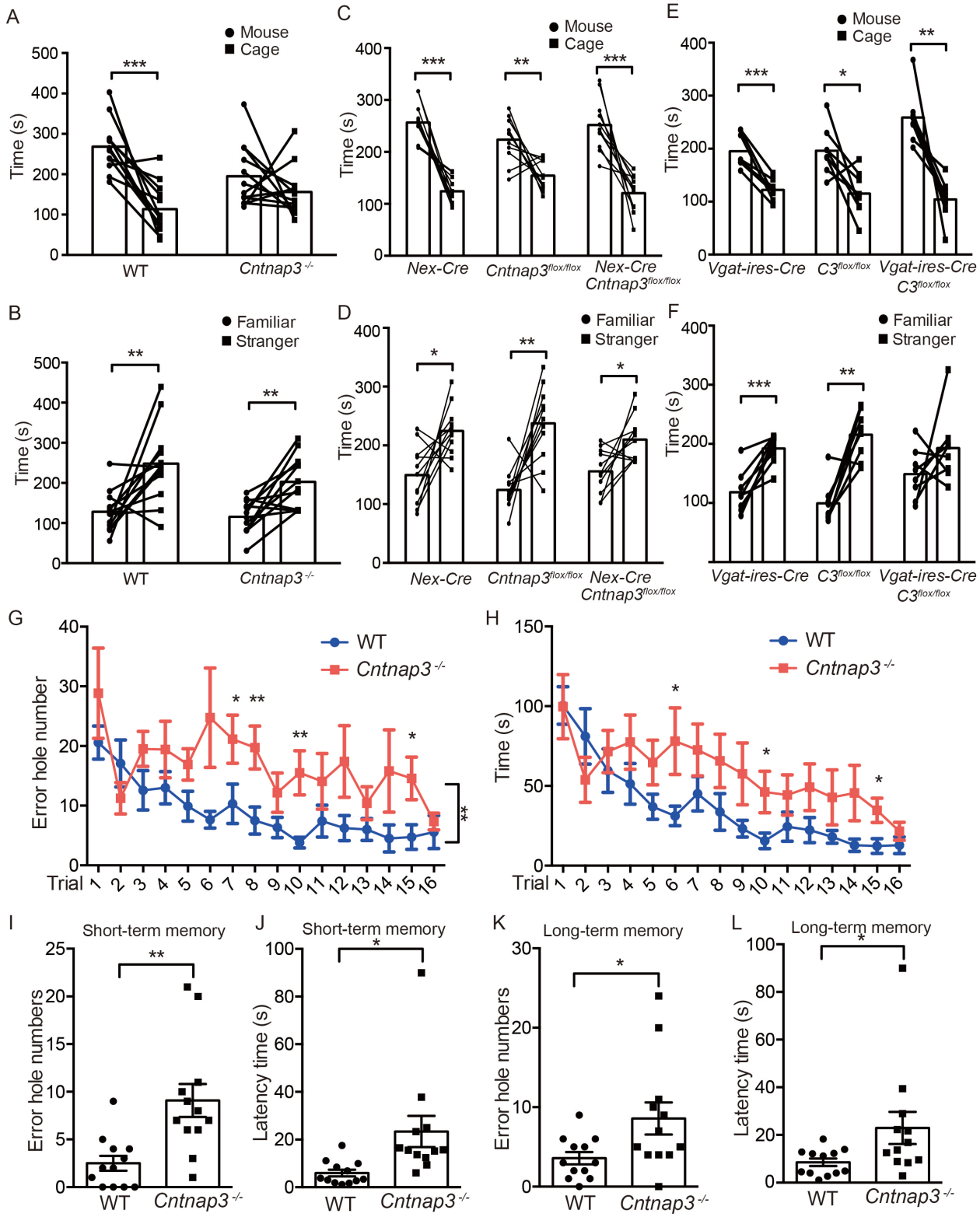

Figure 5. *Cntnap3* KO and conditional KO mice show abnormalities in social behavior and learning memory tasks

Social behaviors in the three-chamber test (A-F), learning and memory task in the Barns maze task (G-L). (A) Time interacting with either an unfamiliar mouse or an empty cage within 10 min. (B) Time interacting with either a stranger mouse or a familiar mouse within 10 min. (n= 12 for either *Cntnap3*$^{-/-}$ or WT mice). (C) Time interacting with either an unfamiliar mouse or an empty cage within 10 min. (D) Time interacting with either a stranger or a familiar mouse in 10 min. (n= 11 for each genotypes). (E) Time interacting with either an unfamiliar mouse or an empty cage within 10 min. (F) Time interacting with either a stranger mouse or a familiar mouse within 10 min. (n= 8 for each genotypes) (G) Learning curve as indicated by the latency time to enter the hole (up to 180 s) during a 4-day training period. (H) Learning curve as indicated by the error hole number before entering the hole during a 4-day training period (n= 12 for either *Cntnap3*$^{-/-}$ or WT mice). The latency time (I) and error hole number (J) before entering the hole (up to 90s) at the first test (short-term memory). The latency time (K) and error hole numbers (L) before entering the hole (up to 90s) at the second test (long-term memory). Statistical significance was evaluated by Student's t test, paired *t* test (3 chamber tests) or two-way ANOVA (curve): *$p < 0.05$, ** $p < 0.01$, *** $p < 0.001$, Error bars, ± SEM.

Supplementary materials

Methods and materials

Figs. S1-S10